Journal of Inorganic Biochemistry 196 (2019) 110686

Contents lists available at ScienceDirect

Journal of Inorganic Biochemistry

journal homepage: www.elsevier.com/locate/jinorgbio

Heme prevents highly amyloidogenic human calcitonin (hCT) aggregation: A potential new strategy for the clinical reuse of hCT

Huixian Ye, Jun Zhou, Hailing Li*, Zhonghong Gao*

Hubei Key Laboratory of Bioinorganic Chemistry and Materia Medica, School of chemistry and chemical Engineering, Huazhong university of Science and Technology, Wuhan 430074, People's Republic of China

ARTICLE INFO

Keywords:
Heme
Human calcitonin
Aggregation
Inhibitor
Hypocalcaemic activity

ABSTRACT

Irreversible aggregation can extremely limit the bioavailability and therapeutic activity of peptide-based drugs. Thus, peptide fibrillation is an excellent challenge for biotechnological drug development. Human calcitonin (hCT) is such a peptide hormone known for its hypocalcaemic effect but has limited pharmaceutical potential due to a high tendency to aggregate. hCT is therefore not widely used preparation in clinical practice. Nonetheless, hCT seems to be still an ideal target for clinical therapy when fibrillation is effectively inhibited, because the alternatives of hCT can stimulate undesirable immune responses in patients and cause side effects. Interestingly, heme is an essential component for many livings and has been shown a strong inhibitory effect on some amyloidogenic peptides aggregation. Here we demonstrate that it may be a most suitable, safe, biocompatible small molecule inhibitor on hCT aggregation, and thereby improving its activity when guiding the drug peptide in clinical therapeutics. In this work, we found that heme was able to reversibly bind with hCT to form a heme-hCT complex with a moderate binding constant ($9.17 \times 10^6\,M^{-1}$) and significantly suppress the aggregation of hCT probably accomplished by heme binding to it, blocking the β-sheet structure assembly which is essential in hCT fibril aggregation. Meanwhile, the heme-hCT complexes showed enhanced bioactivity compared to hCT itself after a 24 h incubation time in reducing blood calcium levels in mice. This study may develop a new strategy to reuse the wild-type hCT in clinical therapeutics.

1. Introduction

Many peptides and proteins with biological activity have been increasingly utilized in therapeutic formulations due to their involvement in various metabolic pathways. Their capability to act as a drug is coupled to a particular conformation and is lost when conformational transition occurs [1]. Therefore, aggregation is a major obstacle for these peptides or proteins, having an intrinsic propensity to aggregate irreversibly, to use in clinical practice. Many peptide-based drugs with great therapeutic potential are restricted to their self-assembling propensity because it cannot only compromise their therapeutic activity but it may also increase the risk of immunogenic reactions [2,3]. Searching and developing proper ways to inhibit the aggregation is thus of great importance for extending their application in clinical therapy.

Human calcitonin (hCT) is a 32-amino-acid peptidyl hormone (primary structure see Fig. 1) produced and secreted by the parafollicular C cells of the thyroid, and participation in the calcium-phosphorus metabolism in our body [4,5]. Its primary structure is characterized by the presence of a disulfide bridge between residues Cys1 and Cys7, and the C-terminal proline amide, which are considered as the key portions for its biological activity [6–8]. Calcitonin acts to decrease blood calcium and phosphate levels, and to reduce bone resorption by inhibiting the activity of osteoclast cells [4,9,10]. For this reason, calcitonins(CTs) have been used therapeutically for the treatment of metabolic bone disorders such as osteoporosis, Paget's disease, hypercalcemia of malignancy and musculoskeletal pain [11–13]. However, the therapeutic application of hCT is extremely limited due to its high intrinsic tendency to assemble into amyloid fibrils, as often observed in many other peptides associated with degenerative disorders like Alzheimer's disease, Parkinson's disease and type II diabetes [14,15]. Amyloid deposits of hCT result in a significant decrease in its activity as a drug and even are closely associated with some diseases [16–18]. A well-known example is “Etiopathology of Human Medullary Thyroid Carcinoma (MTC),” which is the consequence of amyloid fibril deposits formed by hCT [18]. Moreover, aggregation also elicits undesirable immune responses leading to resistance or allergic reactions [19–21] and increases drug-induced cytotoxicity [22]. On the contrary, salmon calcitonin (sCT) has 40–50 times higher potency but shows lower aggregation

* Corresponding authors.
E-mail addresses: lihailing86@hust.edu.cn (H. Li), zhgao144@mail.hust.edu.cn (Z. Gao).

https://doi.org/10.1016/j.jinorgbio.2019.03.026
Received 14 January 2019; Received in revised form 20 March 2019; Accepted 31 March 2019
Available online 01 April 2019
0162-0134/

Fig. 1. the primary structure of human calcitonin.

propensity compared with hCT. This is also the reason that sCT is the most widely used therapeutic preparation in clinical practice despite its 50% homology to hCT [1]. However, the use of sCT has been shown to stimulate immune reactions as well, resulting in side effects such as anorexia and vomiting [23,24]. It has been also reported that sCT produce antibodies in a remarkable number of patients resulting in development of clinical resistance against the non-hCT [25–27]. Interestingly, earlier study has verified that the potency of hCT could be enhanced when the fibrillation is avoided, exhibiting a much higher potency than sCT [28]. These findings indicate that the wild-type hCT is still the most suitable, clinically effective and well tolerated for curing these calcium-related diseases if its aggregation propensity could be significantly reduced. But for a long time, no ideal ways were found to control the aggregation during the production, storage and distribution of hCT and its administration to patients, explaining why hCT has never been largely used as therapeutic. Therefore, it imposes an importance to develop a series of inhibitors that have strong inhibitory effect on hCT aggregation, at the same time, should be safe and biocompatible for pharmaceutical preparation of hCT in vitro and therapeutic application in vivo.

Heme (iron-protoporphyrin) is a co-factor for many living organisms, particularly mammals and involved in multiple physiological processes including oxygen transport and storage, electron transfer, signal transduction, and micro RNA processing [29–31]. It acts as a prosthetic group and plays an essential role in the functions of various types of proteins and enzymes such as hemoglobin and myoglobin, as well as cytochromes, catalase and peroxidase [29,30,32]. In a previous study, heme has been shown to use as therapeutic drug to correct disorders of heme metabolism (e.g., porphyria, various forms of jaundice, and hematological diseases) [33]. Recently, more and more researches indicate that heme can also act as a strong protein misfolding inhibitor, preventing fibril formation for amyloid β-protein, α-synuclein and human islet amyloid peptide (hIAPP), et al. [34–36]. Moreover, it has been revealed that the strong inhibitory effect of heme on amyloid peptide is mainly mediated via the combination of heme with peptide. Actually, heme can interact with those peptides containing some specific amino acid residues or structure regions [36–38], forming a heme-peptide complex, which plays prominent roles in blocking β-sheet structure assembly of aggregated peptide. When these specific amino acid residues or the regions are missing in the peptide sequence, the inhibitory effect of heme on peptide aggregation is significantly reduced or even loss [36,37]. A large number of heme binding site studies have demonstrated that Arg, Tyr and His are these predominant acid residues for heme binding in heme-proteins [39]. Among them, His has been proved to be preferentially bound to heme and it is known as a heme-Fe binding site [40–43]. Intriguingly, hCT also highlights the presence of a histidine residue at the position 20. Thus, it also has the high potential to bind with heme and such binding may significantly prevent the aggregation of hCT. Taken these together, we therefore speculate that the natural compound, heme, may be able to become a safe and biocompatible inhibitor for hCT, reducing its aggregation and thereby enhancing its potency as drug. This will provide not only a novel strategy to control the fibril formation of hCT, but also a possibility for the reuse of hCT in clinical therapy. However, to the best of our knowledge, no work has been reported on this strategy in current studies.

In this work, we for the first time demonstrated that heme can rapidly bind with hCT and such binding has a strong inhibitory effect on hCT aggregation and thereby assist to maintain the physiological activity of hCT in vivo. This finding gives a new direction to improve the bioactivity of hCT in aqueous solution and will have great significance for preparing therapeutic formulations of hCT using for clinical therapy.

2. Materials and methods

2.1. Materials

Human calcitonin (> 95%) were obtained from Chinapeptides (Shanghai, China). Ferriprotoporphyrin IX chloride (hemin, referred to as “heme” hereafter), PP (protoporphyrin), 1,1,1,3,3,3-hexafluoroisopropanol (HFIP), 4,4′-dianilino-1,1′-binaphthyl-5,5′-disulfonic acid (Bis-ANS) and thioflavin T (ThT) supplied by Sigma-Aldrich (St Louis, MO, USA). The sterile saline solution (0.9%, w/v) and bovine serum albumin (BSA) for the hypocalcaemic assay was purchased from Fuxing Bio-Pharmaceutical (Wuhan, China) and Sigma, separately. A Calcium Kit was from Jiancheng Bioengineering institute (Nanjing, China). Unless specified, all other chemicals and materials were of the highest purity commercially available. Deionized water from a Milli-Q system (Millipore, Billerica, MA, USA) was used for solution preparation.

2.2. Sample preparation

For vitro experiments, human calcitonin was dissolved in hexafluoroisopropanol at a concentration of 1 mg/ml, incubated at room temperature for 30 min and sonicated for 1 min in a bath sonicator to ensure consistent monomeric starting conditions. Peptide was then separated into 80 μL aliquots, flash frozen at −80 °C and lyophilized for a period of 24 h. Thereafter, peptide aliquots were stored at −20 °C prior to use. Peptide solutions were prepared by resolubilizing the lyophilized aliquots to desired concentration. The heme or PP stock solution (10 mM) was obtained by dissolving in DMSO and then aliquoted and stored in the dark at −20 °C until use. For in vivo hypocalcaemic assay, the 0.9% sterile saline containing 0.1% (w/v) BSA solution was used as vehicle to prepare injection solutions.

2.3. UV–vis absorption spectroscopy

UV–vis absorption spectrum measurements were performed on a UV 2600 spectrophotometer (Shimadzu Co., Japan) at 25 °C in the range of 300 nm to 800 nm. hCT and heme were dissolved in 50 mM phosphate buffer (PB, pH 7.4) to a final concentration of 20 μM and solutions were then incubated at 37 °C for 30 min. Control experiments were carried out by adding hCT or heme alone into PB. For kinetic study, the spectra were recorded with 20 μM heme as a control immediately after the mixture. The spectrum scanning at corresponding time intervals was repeated till the change of spectra became subtle.

2.4. Electrochemical measurements

Electrochemical properties of heme in the presence of hCT were studied by differential pulse voltammetry (DPV). The DPV experiments were performed on a CHI820D electrochemical workstation (Shanghai Chenhua, China) in a three-electrode cell system with glassy carbon as the working electrode, a platinum wire as the counter electrode, and a saturated calomel electrode as the reference electrode. 100 mM PB (pH 7.4) was used as supporting electrolyte solution. Prior to measurements, the electrolyte solutions were purged with high purity nitrogen gas for 15 min to remove the pre-dissolved oxygen. The following experimental parameters of DPV were used: amplitude, 50 mV;

pulse width, 0.05 s; pulse period, 0.1 s. All tests were carried out at room temperature.

2.5. Isothermal titration calorimetry (ITC)

To determine the binding constant for the interaction between heme and hCT, ITC experiments were performed on a NANO ITC system (TA Instruments Inc., New Castle, Delaware, USA) with a volume of 190 μL sample cell and a maximal 50 μL injection syringe. All titrations were carried out in 10 mM PB, pH 7.4. Heme was dissolved in a minimal volume of 0.1 M NaOH, further diluted to desired concentration with 10 mM PB and centrifuged at 10000 rpm for 5 min. The concentration of heme was measured again using an extinction coefficient value of $\varepsilon_{385} = 58{,}440\ M^{-1}\ cm^{-1}$ [44]. To avoid heme aggregation, heme solutions were freshly prepared prior to the measurements. All solutions were thoroughly degassed under vacuum for 20 min before use. The titration data were obtained from titrating heme (400 μM) at a time interval of 150 s into 20 μM hCT solutions, with stirring at 400 rpm at 25 °C. The experiments consisted of 16 successive injections. The blank titration heat of heme diluted into the PB buffer was subtracted from the titration data. The corrected calorimetric data were analyzed using NanoAnalyze software (TA Instruments Inc.) and were fitted to an independent model, from which the binding affinity value were determined.

2.6. Heme transfer

The reversibility of heme binding to hCT was examined by heme transfer experiment as previously described with minor modifications [45,46]. Briefly, 5 μM hCT samples were pre-incubated with equivalent heme for 30 min at 25 °C. Then, the heme transfer experiments were conducted on UV 2600 spectrophotometer (Shimadzu Co., Japan) by the addition of excess (20 μM) bovine serum albumin. The data were collected at a time interval of 5 min in the range of 300–800 nm.

2.7. Thioflavin T and Bis-ANS fluorescence assay

The kinetics of hCT amyloid formation and the inhibitory effect of heme and PP on its aggregation were mainly monitored by the Thioflavin T (ThT) assay, as an increase in fluorescence emission at 482 nm occurs upon the amyloid-specific dye ThT incorporation into β-sheet amyloid structures [47]. Bis-ANS assay was also performed to further determine the fibrosis degree of hCT in the absence or presence of heme and PP. The fluorescence assay was carried out using RF5301 spectrofluorimeter (Shimadzu Co., Japan). The peptide stock solutions were diluted into working solutions with a final concentration of 20 μM hCT and 20 μM heme or PP in 50 mM phosphate buffer. For the assay, working solutions were diluted again 10- fold into PB with 10 μM ThT or 10 μM Bis-ANS. Samples were monitored over a 48 h period at an excitation wavelength of 450 nm for ThT and 385 nm for Bis-ANS. Each experiment was performed with at least three independent repeats. The fluorescence values were exhibited using mean with bars indicating the SEM.

2.8. Confocal fluorescence microscopy

hCT and hCT with heme or PP samples were observed by confocal fluorescence microscopy after staining with ThT or Bis-ANS. All samples were stained with ThT or Bis-ANS at the same concentration 100 μM immediately prior to measurement. The measurements were performed on a Zeiss LSM 880 confocal laser scanning microscope with a 10× objective. The fluorescence images were collected with an excitation at 450 nm for ThT and 385 nm for Bis-ANS. The concentration of hCT was 20 μM in all samples.

2.9. Nu-PAGE

Nu-PAGE electrophoresis was performed with 4%–12% Nu-PAGE Bis-Tris Protein Gels (Invitrogen) using the Mini Gel Tank device (life technologies). The peptide solutions in the absence or presence of heme and PP taken at different incubation time intervals, i.e., 0, 12, 24 h, were diluted with 4× LDS Nu-PAGE loading buffer to a final concentration of 15 μM. The samples were then loaded onto a 10-well gel and run in MES buffer (pH 7.3) at 200 V for 30 min according to the manufacturers protocol (Nu-PAGE Invitrogen). At the conclusion of the run period, silver staining was used for visualization [36].

2.10. Transmission electronic microscopy (TEM) assay

The samples for TEM observation were prepared by incubating 20 μM hCT solution with or without heme and PP in a pH 7.4 PB for 0 h and 24 h at 37 °C. Then, 30 μL of each sample were allowed to absorb on a 200-mesh copper grid covered by carbon-stabilized Formvar film for 5 min. Thereafter, excess fluid was removed, the grid was negatively stained with 30 μL of 5% uranyl acetate for 10 min and dried in air. Finally, Negative stain images were obtained with a transmission electron microscope (HITACHI H-7000FA) at an accelerating voltage of 75 kV.

2.11. Atomic force microscopy (AFM)

The samples for AFM observation were prepared by incubating 20 μM hCT solution in a pH 7.4 PB for 24 h at 37 °C. 10-μL aliquot of each sample taken at 0 h and 24 h was then dropped on freshly cleaved mica surface, dried at room temperature. The morphology of hCT in the absence or presence of heme and PP were collected with a SPM 9700 instrument (Shimadzu Co., Japan). Each image was acquired in the tapping mode and the scan rate was kept at 1 Hz. To obtain representative images in each case, at least four spots in the entire surface areas were scanned.

2.12. Circular dichroism

Circular dichroism (CD) spectra were obtained on a Jasco J-810 spectropolarimeter (JASCO Corp., Japan) at the room temperature. Spectra were recorded in the range of 190–260 nm with 40 μM hCT in 5 mM PB immediately after preparation and 40 μM hCT in the absence or presence of 10 μM heme and PP after incubation for 24 h. Measurements were carried out in a 1 mm path length cell with the scan speed set at 500 nm/min and a spectral bandwidth of 1 nm. Each sample spectrum was corrected using the blank spectrum of buffer. Three scans were averaged, and the spectral results are reported as ellipticity (mdeg).

2.13. In vivo hypocalcaemic assay

The method used for this experiment was based on previous reports of hypocalcaemic potencies of calcitonin in mice after subcutaneously injection with minor modification [48]. Briefly, female KM mice at 8 weeks of age were injected subcutaneously in the dorsal neck with 2 μg dose of hCT in the absence or presence of equimolar heme incubated for 0 h and 24 h in 300 μL 0.9% (w/v) sterile saline containing 0.1% (w/v) BSA. Control mice were injected with an equal volume of the BSA/saline solution without peptide. To gain insight into the effect of heme on the level of calcium, the BSA/saline solution containing only heme was also injected into a group of mice. Blood was collected by fundus venous plexus before the treatment and after 1 h injection, separately. Thereafter, blood was placed at 37 °C for 1 h, centrifuged at 3000 rpm and 4 °C for 20 min, and the serum was then collected. The levels of serum Ca^{2+} were determined using a colorimetric method (A_{610}) with a Calcium kit. Hypocalcaemic activities of corresponding

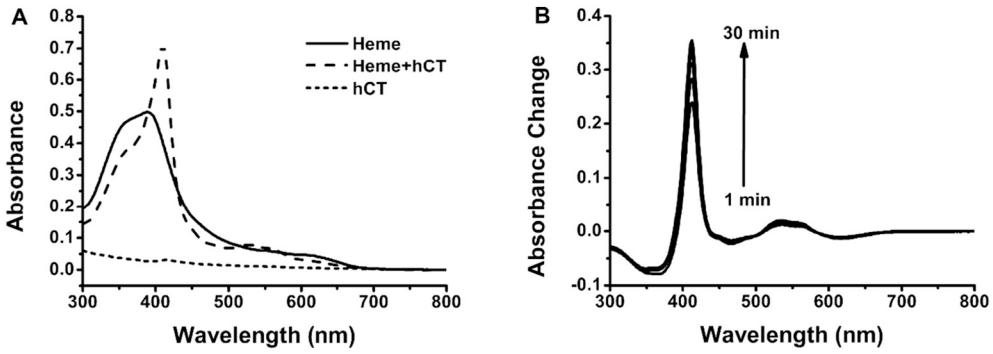

Fig. 2. (A) The spectral change of heme induced by hCT. (B) Kinetic study of the intermolecular interaction between heme and hCT. The absorption spectral data were all recorded in 50 mM phosphate buffer (pH 7.4) with the peptide concentration of 20 μM and/or equimolar heme. For kinetic study, the absorption spectrum obtained at different time intervals were detected using heme as a control.

injection solutions were derived from the [Ca^{2+}] levels change between pre and post-treatment and were plotted as percentage reduction of [Ca^{2+}] (mean ± SEM) relative to pre-treatment calcium contents.

2.14. Statistical analysis

The results are expressed as the mean ± SEM of at least triplicate experiments. One-sample *t*-Test was used for statistical analyses and the difference in P values < 0.05 were considered significant.

3. Results

3.1. Heme directly bound to hCT

It has been well known that the absorption spectrum of heme could be changed upon binding with peptides [40]. Therefore, to exam the intermolecular interaction between hCT and heme, the absorption spectrometry was firstly applied here. We found that the absorption spectrum of heme in the presence of hCT exhibited an obvious red shift from 390 nm to 408 nm relative to heme alone and the intensity of it soret band was remarkably enhanced (Fig. 2A). These observations implied that there existed a strong interaction between heme and hCT and heme was easily to bind with hCT. The large redshift in the heme spectrum indicates that the iron moiety of heme is involved in the combination to hCT. Histidine is viewed as the most likely amino acid to mediate this interaction.

The kinetic study spectrum was recorded immediately after hCT was added to heme solution. As shown in Fig. 2B, the UV–vis absorption of hCT-heme complex rapidly increases at 408 nm once the addition of hCT and the absorption at 408 nm did not increase further when the reaction time reached 30 min. This result indicated that the interaction between hCT and heme was instantaneous and this process needs only about 30 min, implying the extremely strong interaction between hCT and heme.

DPV is a rapid and convenient method to detect subtle changes in redox properties of the electroactive species reflecting their interactions [49,50]. Thus, the ability of heme to interact with hCT was also observed via DPV measurements. As shown in Fig. 3, free heme had a good redox activity and a well-defined reduction peak location at −0.38 V was clearly observed. After incubation with hCT, the reduction peak potential of heme shifted from −0.38 V to about −0.44 V.

It means that reduction of heme in the presence of hCT is more difficult than that the reduction of free heme. Moreover, the reduction peak currents of heme was remarkably reduced during the process and reached a steady state within about 30 min. Together, these results indicated that heme could bind with hCT in complex form, and forming such a stable complex took about thirty minutes. This accords approximately with the UV–vis data, further confirming the close correlation between heme and hCT molecules.

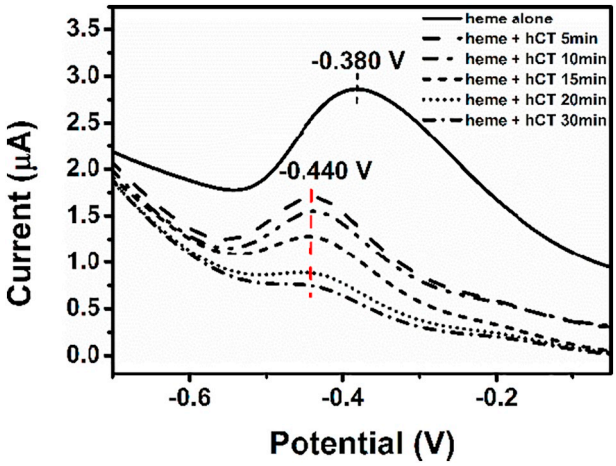

Fig. 3. Time-dependent changes of electrochemical properties of heme (1 μM) in the presence of equimolar hCT as demonstrated by DPV.

3.2. Heme binding affinity and reversibility

To further detect the ability of heme binding to hCT, we used isothermal titration calorimetry as well to determine the binding affinity between heme and hCT. The representative binding isotherm of heme and hCT was shown in Fig. 4A. The result showed that heme could bind to hCT with an association constant value (Ka) of $9.17 \times 10^6\ M^{-1}$. This value clearly revealed that there was a direct and strong interaction between heme and hCT, also further confirming the result obtained from UV and DPV tests. However, it was also worth noting that this value was obviously lower than that between heme and Serum albumin, with an association value up to $\sim 10^8\ M^{-1}$ [51]. Therefore, it is easily to understand that such interaction will be destroyed by the presence of serum albumin or higher affinity protein, such as apomyoglobin, hemopexin et al. [46,52]. To verify this, we also performed a heme transfer experiment generally by monitoring the increase of absorbance at 409 nm after the addition of excess apomyoglobin to heme-binding protein [45,46]. Herein, we used an alternate, BSA with the lower binding affinity than apomyoglobin but being the most abundant protein in serum to carried out this experiment. As shown in Fig. 4B, a spectral red shift occurred from 408 nm to 410 nm and the absorbance intensity at 410 nm were significantly increased. Both the 2 nm shift and the increase in absorbance were characteristics of heme-BSA complexes formation, suggesting the heme transferred from hCT to BSA due to its higher binding affinity. This result also implies that this binding between heme and hCT is reversible after administration to body.

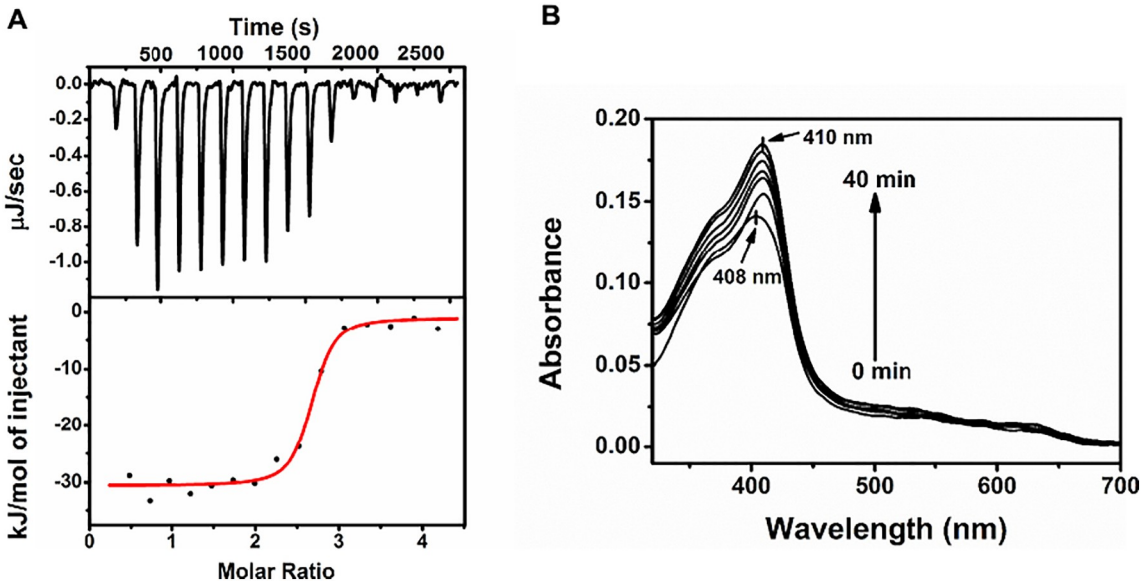

Fig. 4. (A) ITC data for the interaction between heme and hCT in 10 mM PB at 25 °C (B) Absorbance spectrum of 5 μM heme-hCT complex supplemented with 20 μM BSA for 40 min.

3.3. Aggregation kinetics of hCT as demonstrated by ThT and Bis-ANS fluorescence assay

It is widely accepted that an increase in ThT fluorescence intensity at emission wavelength of 482 nm is indicative of the formation of amyloid-like structures enable ThT binding [47,53,54]. Therefore, to characterize the effect of heme in the amyloid aggregation of hCT, the kinetic behaviours of fibrillation at pH 7.4 were investigated in the presence of heme, as detected by ThT fluorescence assay. As shown in Fig. 5A, hCT showed a significant increase in fluorescence values that reached the plateau stage after about 20 h incubation, suggestive of a rapid fibrillation.

process, which was in agreement with previous findings [53]. However, in the presence of heme, hCT did not show any increase in ThT fluorescence and always exhibited low fluorescence values during the whole experiment time (48 h). As a comparison, we also added PP, a surrogate of heme, to observe its effect on hCT aggregation. It also showed the strong inhibitory effect on hCT aggregation, but which was weaker in comparison with heme. These results indicated that, under the conditions of this experiment, heme completely inhibited the formation of amyloid fibril of hCT and this effect was most likely mediated via the interaction between both the iron center and porphyrin ring of heme with hCT.

The final thioflavin-T fluorescence intensity is closely correlated to the amount of fibrillary material formed, the binding constant for thioflavin-T and the quantum yield of the bound dye [55,56]. Differences in thioflavin-T fluorescence intensity between different samples are often attributed to the amount of amyloid formed. However, the latter two factors may also contribute to any observed differences. To avoid the false positive result, it is important to directly confirm the formed aggregates under above conditions. Interestingly, fluorescence microscope can help us directly observe the formed aggregates upon binding with ThT dye [8]. Therefore, we applied fluorescence microscopy to confirm the result obtained from fluorescence spectroscopy. Fig. 5B shows the fluorescence microscopy images of hCT in the presence of heme or PP after 0, 12 and 24 h of incubation at 37 °C. At the beginning of incubation, no aggregates were detected in all samples. After 12 h, some small aggregates emerged in hCT samples; no

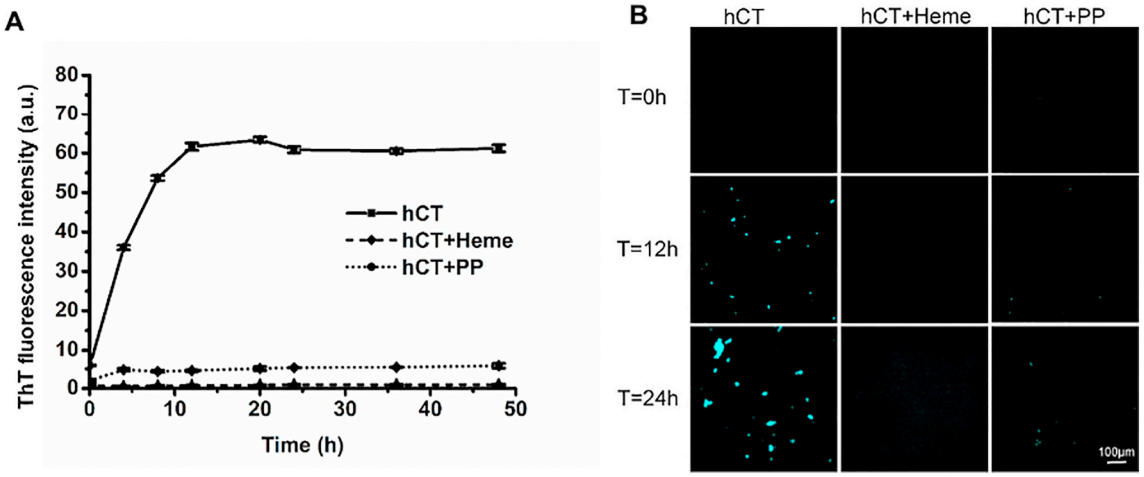

Fig. 5. (A) Kinetics of fibril formation monitored by ThT fluorescence of hCT in 50 mM phosphate buffer at pH = 7.4 and 37 °C without or with heme. PP was performed as a compared group. The inhibitory effect of heme or PP on hCT peptide aggregation was both presented. (B) ThT fluorescence microscopy image of hCT samples at different systems in 50 mM PB pH 7.4 at time 0 h and after 12 h and 24 h incubation at 37 °C.

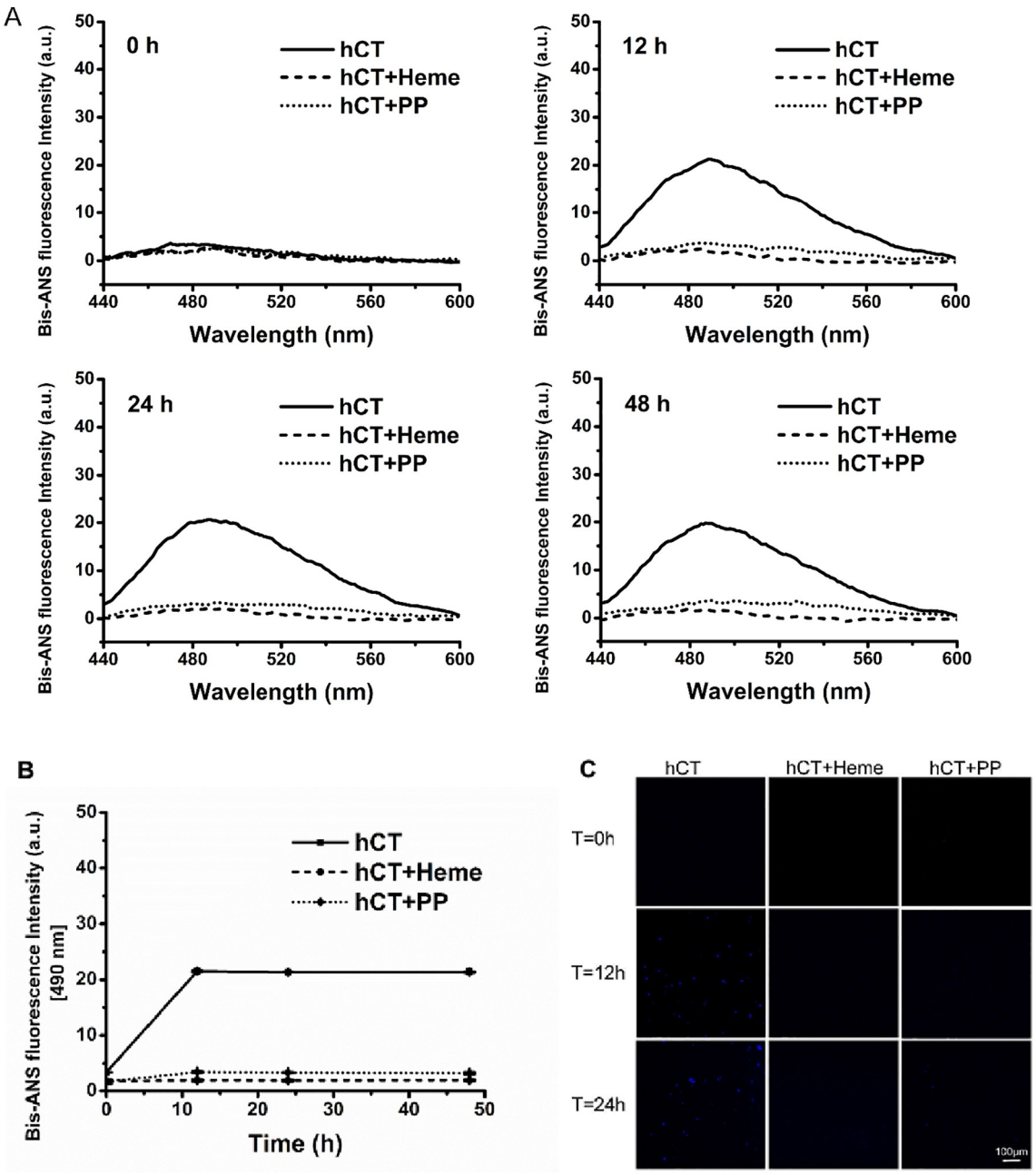

Fig. 6. Aggregation of hCT detected by Bis-ANS assay. (A) Bis-ANS fluorescence spectrum of hCT aggregation in the absence or presence of heme and PP at different points of time. (B) Time course of Bis-ANS fluorescence intensity at 490 nm of hCT, hCT-heme mixture, hCT-PP mixture. (C) Bis-ANS fluorescence microscopy pictures of different hCT samples in 50 mM PB pH 7.4 after 0, 12 and 24 h incubation at 37 °C.

aggregates were detected when heme or PP was added. Incubation at 37 °C for 24 h induced more and larger aggregates formation in the hCT alone samples. However, hCT samples in the presence of heme still did not show any aggregates. In contrast, there were little aggregates in hCT samples with PP. This result was in good agreement with the ThT fluorescence spectroscopy studies, indicating the final thioflavin-T fluorescence intensity was indeed due to the formation of amyloid structure.

To further confirm the observations obtained from the ThT measurement, the Bis-ANS assay was also applied to study the effect of heme and PP on hCT aggregation. Bis-ANS is a hydrophobic fluorescent probe that is widely used in protein folding studies, using their capacity to bind to hydrophobic regions on proteins, and in turn leading to an increase in fluorescence [36,57]. The spectra obtained upon direct excitation of Bis-ANS and the fluorescence intensity at 490 nm as a function of time is shown in Fig. 6**, A** and **B**, respectively. The results were well in accordance with that obtained in ThT fluorescence assay. As expected, the Bis-ANS fluorescence microscope result (Fig. 6C) further supported the fluorescence data. These results indicated that heme indeed had a strong inhibitory effect on hCT aggregation and both its porphyrin ring and iron center played a crucial role in the process of hCT aggregation.

3.4. Oligomerization studies by Nu-PAGE analysis

The oligomerization state of hCT in the presence of heme and PP was also monitored by Nu-PAGE analysis. The result for sample solutions at the desired periods time (0 h, 12 h, 24 h) are presented in Fig. 7. In all samples, the predominant band around 3.4 kDa corresponding to the monomer was observed immediately after sample preparation (0 h).

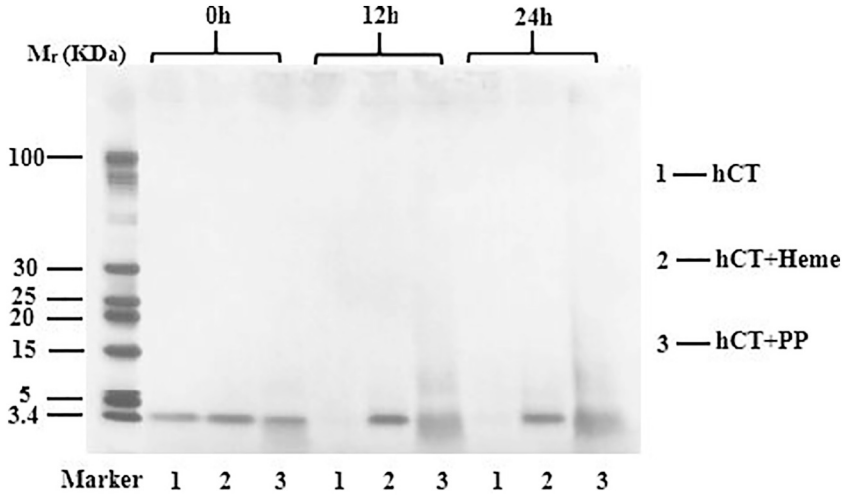

Fig. 7. The effects of heme and PP on hCT oligomerization. 20 μM hCT in the absence or presence of equimolar amounts of heme and PP were incubated in phosphate buffer (50 mM, pH 7.4) at 37 °C for time intervals at 0, 12, 24 h and then analyzed by Gel electrophoresis. 1, 2, 3 represents hCT, hCT + heme, hCT + PP respectively.

For hCT alone, the monomer band disappeared after 12 h incubation, indicating that hCT had been completely transferred into large aggregates or fibrils. However, in the presence of equimolar amounts of heme, the majority of hCT was still maintained to its monomer forms after incubating for 12 h, even 24 h and no oligomers were observed. Compared with heme, the monomer band of hCT decreased slightly with increasing incubation times in the presence of PP. Meanwhile, a small amount of oligomers was also detected during the incubation. These results demonstrated that heme inhibited the oligomer formation and subsequent transformation into large species or fibrils and the inhibitory effect of PP was weaker in comparison with heme.

3.5. Transmission electron microscopy determination of the structure of hCT aggregates

To visually probe the morphology of aggregates formed, the hCT samples incubated for 0 h and 24 h at 37 °C were analyzed by TEM images. The TEM results were found to be in good agreement with ThT fluorescence assay and Nu-PAGE results described above. The TEM images of all samples at different time points are shown in Fig. 8 and clearly indicate that heme significantly affect hCT fibril formation. It was apparent that no significant aggregates were observed at the beginning for each sample. After 24 h of incubation, hCT grew into massive and crowded mature amyloid fibrils, similar to the result reported previously [53]. However, the aggregation degree in the presence of heme is totally different. No any fibril structures are observed after incubation for 24 h. Instead, as shown in Fig. 8B, the image is consisted of just a few small nonfibrilar structures. In contrast, although the hCT sample in the presence of PP showed no fibril formation, it exhibited the rare appearance of short protofibrils and a large amount of amorphous aggregates. The inhibitory effect of PP was obviously weaker than that of heme. These data give a visual evidence that heme significantly suppress the fibril formation of hCT.

3.6. Morphological characterization of hCT aggregates visualized by AFM

Atomic force microscopy (AFM) is a non-invasive and chemical-free imaging technique which has emerged as a promising tool for

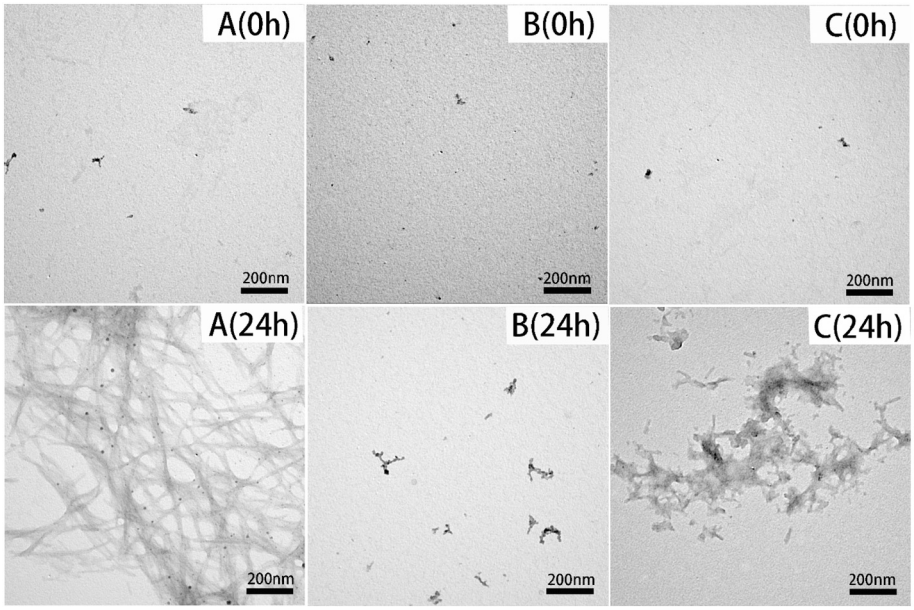

Fig. 8. Transmission electron micrographs of negatively stained hCT in the absence or presence of heme and PP after 0 h and 24 h. A, hCT; B, heme + hCT; C, PP + hCT. All samples were negatively stained with 5% uranyl acetate. Scale bar represents 200 nm.

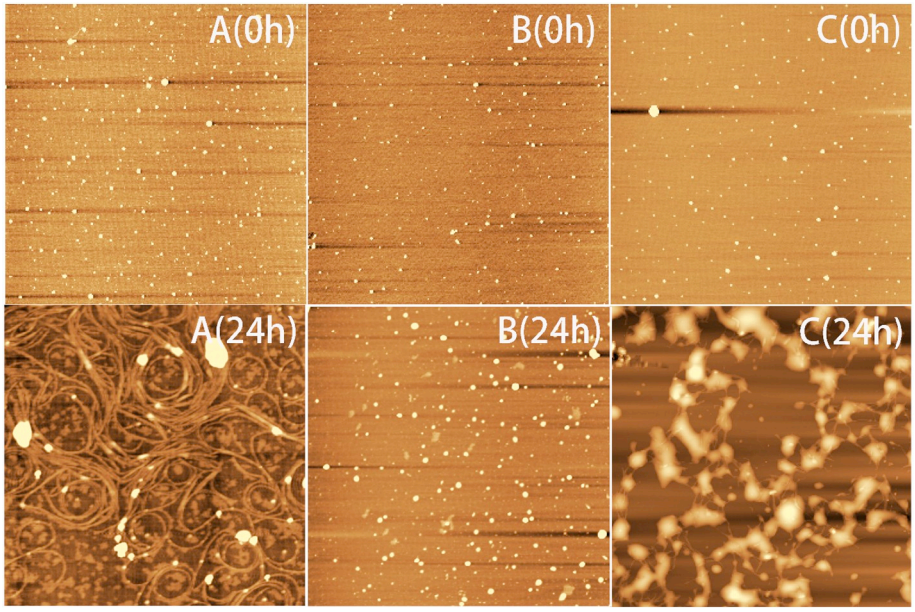

Fig. 9. AFM images of hCT aggregates in the absence or presence of heme and PP. The hCT aggregates were obtained by incubating freshly prepared hCT (20 μM) in 50 mM phosphate buffer (pH 7.4) (A) hCT alone, (B) with 20 μM heme or (C) with 20 μM PP at 37 °C for 0 and 24 h. The size of all images correspond to 4 μm × 4 μm.

investigating nanoscale morphological features of peptide amyloid [58,59]. To further get insight into the morphological differences of hCT aggregates formed in the absence or presence of heme and PP, AFM imaging was performed as well. Images obtained from AFM topographs of aliquots of hCT without or with heme and PP taken at indicated time are shown in Fig. 9. As expected, all the hCT samples showed mostly a few oligomers immediately after preparation (0 h). after 24 h incubation, hCT aggregated to form numerous long, thick, stacked mature amyloid fibrils. However, a 24 h incubation with heme resulted in only the formation of few globular aggregates, no any protofibrils or fibrils were observed. As a comparison, a few protofibrils appeared together a large number of amorphous aggregates in the presence of PP. These observations were similar to the results obtained from the TEM images.

3.7. CD studies of the aggregation of hCT

The structural changes of hCT after fibril formation were also monitored using CD spectroscopy. At 0 h (Fig. 10), hCT owned a predominant random coil conformation, indicated by the minimum negative absorption intensity at 200 nm. Such a monomeric component disappeared after 24 h as a result of fibril formation, corresponding to the huge increase in fluorescence values (Figs. 5 and 6), hCT showed a typical β-sheet conformation with a maximum and minimum ellipticity value at 200 and 222 nm, separately. However, in the presence of heme or PP, hCT still preserve its structure after 24 h incubation though the content of random coil decreased slightly. These results implies that heme can significantly prevent hCT from forming amyloid fibril and keep hCT as its monomeric conformation for a relatively long time (24 h). Also, a slightly stronger inhibitory effect of heme than PP was observed.

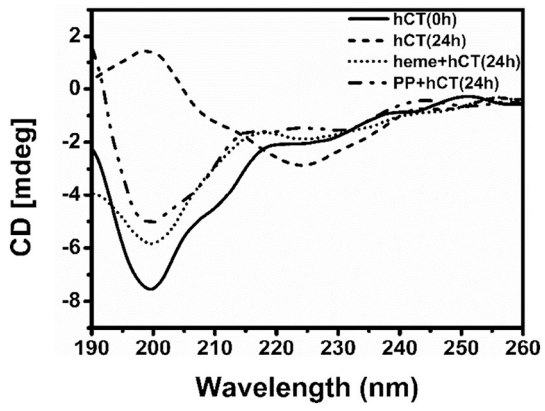

Fig. 10. CD spectroscopy detected the secondary structure transition of hCT without or with heme and PP after incubation for 24 h.

3.8. The effect of heme on hCT hypocalcaemic potency

The hypocalcaemic role of hCT in vivo is strongly associated with inhibition of bone resorption, thus accounting for the pharmacological importance of CTs [60]. It is generally the most direct measurement of hCT bioactivity [48,60,61]. To directly investigate the effect of heme on the maintenance of hCT biological activity, we performed hypocalcaemic potency assay in mice. The result obtained from different injection solution systems is shown in Fig. 11. As expected, hCT at 0 h

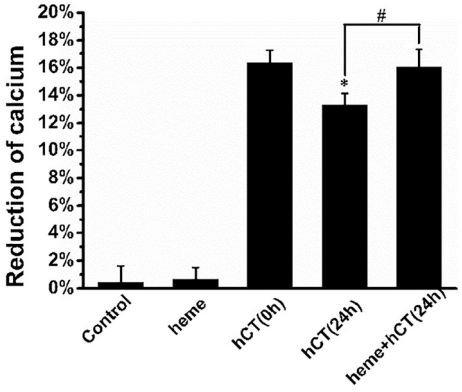

Fig. 11. The effect of heme on hCT hypocalcaemic activity. Serum calcium levels were measured pre and post-treatment of the peptide solution or vehicle alone in groups of 6 mice. Hypocalcaemic potencies for each group are expressed as percentage reduction of calcium (mean ± SEM) obtained by data normalized against pre-treatment. *P < 0.05 in comparison with hCT incubated for 0 h. #P < 0.05 compared with hCT co-incubated with heme for 24 h.

showed well described hypocalcaemic activity. 2 μg dose of hCT caused a 16.3% of calcium reduction, which was similar to the result acquired by Kapurniotu et al. [48]. However, when injected with hCT solution pre-incubated for 24 h, the hypocalcaemic effect of it was decreased significantly. Whereas in the presence of heme, the co-incubation solution of hCT and heme for 24 h still exhibited a potency that was nearly identical to hCT at 0 h. It should be noted that heme alone had no effect on the serum calcium levels in mice. This result indicated that the addition of heme into hCT could help to maintain its biological activity.

4. Discussion

Owing to the high aggregation tendency and low potency of human hormone, sCT is the predominant CT utilized therapeutically for the treatment of osteoporosis, Paget's disease and other hypercalcaemia-related diseases [60]. However, while sCT is the most potent native human calcitonin analogue, it exhibits only 50% sequence homology to hCT, a fact that most probably accounts for the immunological side reactions observed in sCT-treated patients [10,60]. Therefore, the development of a potent inhibitor reducing native human hormone aggregation is still an attractive strategy to the therapeutic use of hCT.

For amyloidogenic peptide or proteins, a number of compounds have been screened or designed as inhibitor [62,63], among which polyphenols like flavonoids and their derivatives have been largely reported [64,65]. More recently, an increasing number of studies indicates that heme, a natural compound, could also prevent amyloid fibril formation of kappa-casein [35], amyloid beta peptide [66], a-synuclein [34] and hIAPP [36] and degrade partially formed amyloid fibrils. These recent discoveries led us to propose that heme may play an important role in reducing the hCT aggregation tendency and thereby enhancing its bioactivity when using heme as a chaperone-like molecule. In this work, the effect of heme on the amyloid fibril formation of hCT was reported for the first time. We found that heme could effectively inhibit the aggregation of hCT using multiple different analytical techniques. The kinetic traces of ThT and Bis-ANS fluorescence absorbance was firstly monitored in the absence or presence of heme. The shapes of fluorescence data (in the presence of heme, Fig. 5 and Fig. 6) shows a dramatic decrease in intensity, which are similar to that observed for other amyloid systems [34,47], suggesting the decrease in the level of amyloid assembles. A similar inhibitory effect was also observed in the following gel electrophoresis (Fig. 7), TEM (Fig. 8), AFM (Fig. 9) and CD (Fig. 10) detection.

To investigate the possible inhibitory mechanism of heme, PP (a surrogate of heme) was applied as comparison experiments. They are all organic protoporphyrin macrocycles and the only difference is an iron atom being included in the center of heme (Fig. 12A). In this study, a remarkable prevention of aggregation of hCT by PP was also presented. It implies that the porphyrin macrocycle has a large contribution to suppress the formation of hCT aggregates. It is generally acknowledged that amyloid fibril formation is mainly driven by hydrophobic and aromatic interactions [67–70], and disrupting such interactions may thus suppress amyloid aggregation. Many previous studies have shown that the interactions of aromatic residues in the residue 9–22, especially between the side chain of Phe16 and Phe19 residues, play prominent roles in fibrillation of hCT [68,71–74]. Moreover, NMR experiments [75] reveal that the interaction of aromatic rings of epigallocatechin gallate (EGCG) with the aromatic side chains of peptide destroy hCT intermolecular π- π stacking, thereby inhibiting fibril formation of hCT. Consequently, it can be expected that the competing interaction of porphyrin macrocycle for theses side chains blocks potential sites for peptide association and prevents fiber formation. However, it should be noting that the inhibitory effect of PP was weaker in comparison with heme. Our UV–vis and DPV data reveal that heme could rapidly bind with hCT to form a heme-hCT complex, showed by the spectra and electrochemical property changes of heme (Fig. 2 and Fig. 3). This interaction is most probably mediated by the nitrogen atom of imidazole group of histidine side chain binding to the iron center of heme. Generally, this binding site in the combination of peptide and metal ions can be identified by using peptide mutant where His is replaced by other residues such as Ala [47,76]. It was found that the absence of His prohibited metal ions binding to peptide, indicating His is a key binding site. Meanwhile, Bondarenko et al. [77] and Bertini et al. [78] also found that His was a common ligand for the active site of metalloproteins in study the structure of paramagnetic metalloproteins such as human cytoglobin and Copper-Nickel superoxide dismutase using NMR technique according to residues shift and relaxation caused by paramagnetism. These studies reveal the prevalence of His in binding to metal ions like heme, copper ions. Therefore, His residue of hCT in this work was also supposed to be the heme binding site. Herein, we can conclude that the complexation of heme with hCT play a crucial role in inhibiting its fibril formation though not essential. Of course, it is also worth noting that some protofibrils still emerged after incubating with PP for 24 h, whereas heme could significantly prevent amyloid fibril formation, observed from the TEM, AFM images. These results confirm the importance of electrostatics between heme and hCT. Taken all these into account, it can be speculated that the strong inhibitory effect of heme on hCT aggregation is accomplished by its porphyrin macrocycle and complexation with hCT, blocking the side chains association of peptide and this possible inhibitory mechanism can be simply reflected in Fig. 12B.

Cudd et al. had shown that the potency of human calcitonin was enhanced when fibrillation was avoided by osteoclast cell experiments [28]. This finding has important implications for human therapy by reusing hCT and therefore lead us the further study on the bioactivity of hCT in the presence of heme. The hypocalcaemic assay in vivo is the only assay approved for determination of bioactivity of calcitonin by health authorities [10,60]. Therefore, we routinely used the hypocalcaemic assay to probe hypocalcaemic potency differences of hCT in the absence or presence of heme at the beginning of preparation and after 24 h, and to evaluate its pharmacological potential in the presence of heme. The obtained data (Fig. 11) revealed that the well effect of heme on hCT bioactivity maintenance. In the presence of heme, the hypocalcaemic potency of hCT even though at 24 h was still identical to that of it upon preparation. Taken all these results together, it could be well speculated that the presented good activity of hCT in the presence of heme at 24 h was most likely due to the strong inhibitory effect of heme on hCT fibril assembly via the complexation, keeping hCT as an active monomeric conformation for a long time. In heme binding affinity experiment (Fig. 4A), we used ITC to obtain the affinity constant between heme and hCT and found it was $9.17 \times 10^6\,M^{-1}$. It implied that this interaction of heme binding to hCT could be destroyed by high heme binding protein, such as serum albumin ($\sim 10^8\,M^{-1}$). Although the binding process of heme with equivalent hCT is kinetic and it takes about 30 min to form stable complexes, as shown in UV and DPV results, the titration heat was successively collected at a time interval of 150 s under the [hCT] > [heme] or [heme] > [hCT] conditions. The binding under such conditions will be rapidly. Moreover, the titration heat curve fell back to baseline during the titration duration (Fig. 4A), which indicated that the reaction between heme and hCT reached equilibrium under above-mentioned conditions. Therefore, this value can be applied to reveal the affinity between heme and hCT. To verify this, we also performed the heme transfer experiment (Fig. 4B). The result demonstrated that heme indeed could be transferred from the heme-hCT complex to a higher binding affinity protein, indicating the rationality of the affinity value obtained in ITC. Accordingly, we believe that when the heme-hCT co-incubation solutions are injected into the mice, heme can be captured by high heme affinity protein and does not interfere with the receptor/ligand interaction in body. This interaction, in turn, enables hCT as a heme-hCT complex to avoid the intermolecular aggregation after preparation in vitro, and released as an active monomer in vivo, thereby maintaining peptide bioactivity. This

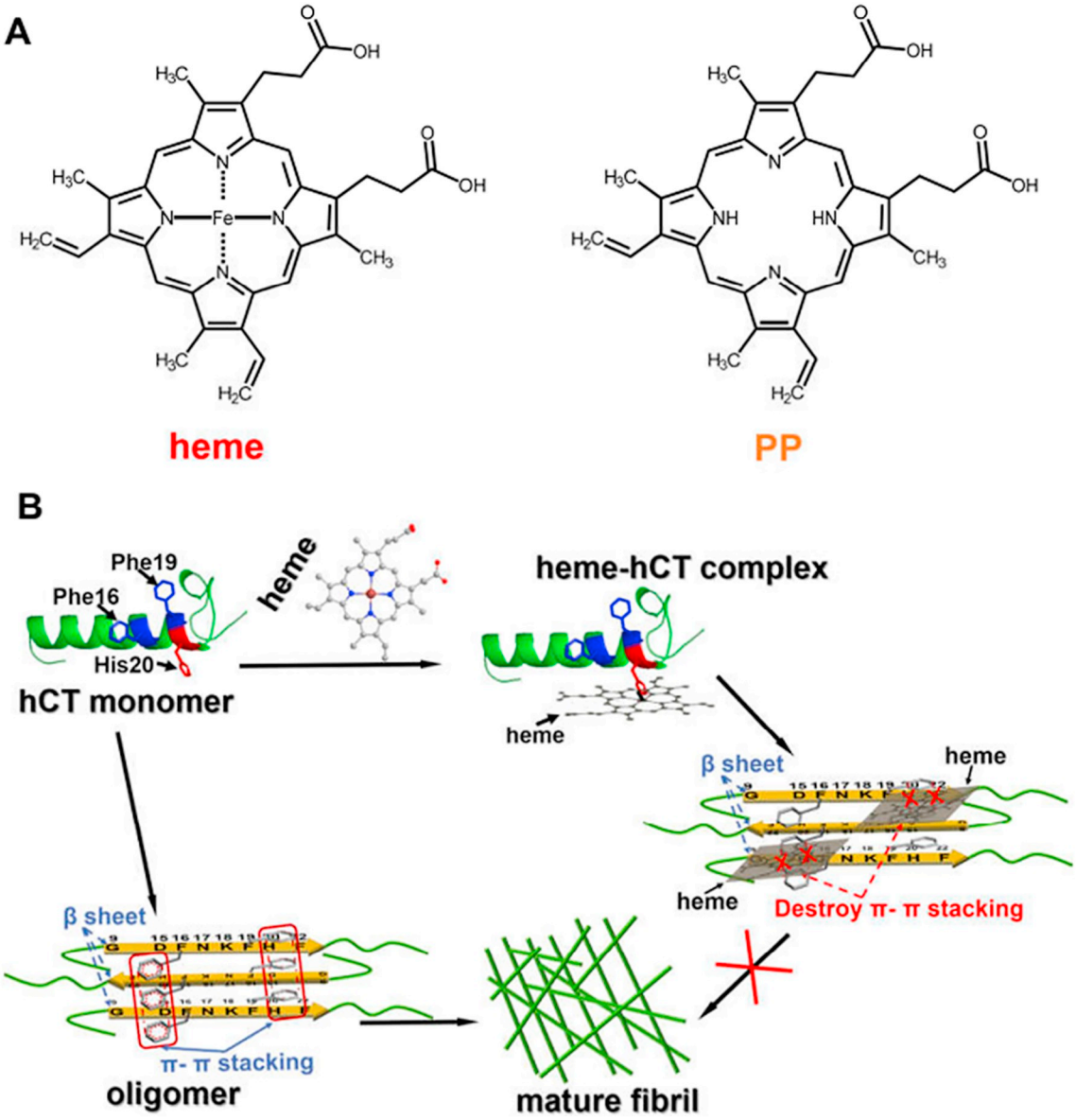

Fig. 12. (A) Chemical structure of heme and PP. (B) Schematic representation of proposed model for the inhibition of fibril formation of hCT by heme. The intermolecular aromatic interaction in the residue 9–22, especially between the side chain of Phe16 and Phe19 residues, was thought to play crucial roles for the hCT fibrillation. Heme can bind with hCT most likely via the His20 residue, adjacent to the Phe19 residue, thereby destroying the intermolecular π-π stacking between hCT molecules and inhibiting its fibril formation.

will be of great significance for the storage, administration and reuse in clinical of this peptide.

5. Conclusion

In summary, we have applied UV–vis, DPV and ITC techniques to demonstrate that hCT can bind with heme to form a hCT-heme complex with a binding constant value of $9.17 \times 10^6\,M^{-1}$. Moreover, the following heme transfer experiment reveals that the heme binding is reversible. Thereafter, we show that such binding can significantly inhibit the fibrillation of hCT, and more importantly, enhance the activity of it as drug compared with hCT alone incubated for a long period of time. This finding provides not only a novel way to prevent the aggregation of hCT, but also a promising strategy to prepare a therapeutic formulation of hCT. Meanwhile, it further confirms the conclusion that heme has a strong inhibitory effect on amyloidogenic peptides misfolding and may be used to prevent the aggregation of other peptide drugs with the potential of forming amyloid aggregates.

Abbreviations

hCT	human calcitonin
sCT	salmon calcitonin
MTC	medullary thyroid carcinoma
hIAPP	human islet amyloid peptide
PP	protoporphyrin
HFIP	1,1,1,3,3,3-hexafluoroisopropanol
Bis-ANS	4,4′-dianilino-1,1′-binaphthyl-5,5′-disulfonic acid
ThT	thioflavin T
BSA	bovine serum albumin
DPV	differential pulse voltammetry
ITC	isothermal titration calorimetry
TEM	transmission electron microscopy
AFM	atomic force microscopy
EGCG	epigallocatechin 3-gallate

Conflict of interest

The authors declare no competing financial interest.

Acknowledgements

This work was supported by the National Natural Science Foundation of China (no. 31770866 and 31570810) and the Natural Science Foundation of Hubei Province Scientific Committee (2016CFA001). Wuhan Institute of Virology, Chinese Academy of Sciences is thanked for its help with the TEM imaging. We also thank professor Fan Xia for supplying the confocal microscope instrument and Mr. Xudong Wang for his technique assistance in collecting fluorescence microscope images.

References

[1] N. Rastogi, K. Mitra, D. Kumar, R. Roy, Inorg. Chem. 51 (2012) 5642–5650.
[2] E.Y. Chi, S. Krishnan, T.W. Randolph, J.F. Carpenter, Pharm. Res. 20 (2003) 1325–1336.
[3] H. Schellekens, Nat. Rev. Drug Discov. 1 (2002) 457.
[4] L.A. Austin, H. Heath, New Engl. J. Med. 304 (1981) 269–278.
[5] D.H. Copp, B. Cheney, Nature 193 (1962) 381–382.
[6] R. Neher, B. Riniker, R. Maier, P.G.H. Byfield, T.V. Gudmundsson, I. MacIntyre, Nature 220 (1968) 984.
[7] B. Riniker, R. Neher, R. Maier, F.W. Kahnt, P.G. Byfield, T.V. Gudmundsson, L. Galante, I. MacIntyre, Helv. Chim. Acta 51 (1968) 1738–1742.
[8] F. Mulinacci, E. Poirier, M.A. Capelle, R. Gurny, T. Arvinte, Eur. J. Pharm. Biopharm. 78 (2011) 229–238.
[9] T.J. Chambers, J. Cell Sci. 57 (1982) 247–260.
[10] T. Chambers, C. Magnus, J. Pathol. 136 (1982) 27–39.
[11] M.C. Gaudiano, M. Colone, C. Bombelli, P. Chistolini, L. Valvo, M. Diociaiuti, Biochim. Biophys. Acta 1750 (2005) 134–145.
[12] N. Mehta, A. Malootian, J. Gilligan, Curr. Pharm. Des. 9 (2003) 2659–2676.
[13] J.M. Lane, Spine 22 (1997) 32S–37S.
[14] M. Stefani, C.M. Dobson, J. Mol. Med. 81 (2003) 678–699.
[15] A.S. DeToma, S. Salamekh, A. Ramamoorthy, M.H. Lim, Chem. Soc. Rev. 41 (2012) 608–621.
[16] S.B. Fowler, S. Poon, R. Muff, F. Chiti, C.M. Dobson, J. Zurdo, Proc. Natl. Acad. Sci. U. S. A. 102 (2005) 10105–10110.
[17] M. Zaidi, A. Inzerillo, B. Moonga, P. Bevis, C.-H. Huang, Bone 30 (2002) 655–663.
[18] R. Khurana, A. Agarwal, V.K. Bajpai, N. Verma, A.K. Sharma, R.P. Gupta, K.P. Madhusudan, Endocrinology 145 (2004) 5465–5470.
[19] D. Schubert, C. Behl, R. Lesley, A. Brack, R. Dargusch, Y. Sagara, H. Kimura, Proc. Natl. Acad. Sci. 92 (1995) 1989–1993.
[20] A. Braun, L. Kwee, M.A. Labow, J. Alsenz, Pharm. Res. 14 (1997) 1472–1478.
[21] J. Brange, L. Andersen, E.D. Laursen, G. Meyn, E. Rasmussen, J. Pharm. Sci. 86 (1997) 517–525.
[22] D.L. Rymer, T.A. Good, J. Biol. Chem. 276 (2000) 2523–2530.
[23] Y. Yamamoto, H. Nakamuta, M. Koida, J.K. Seyler, R.C. Orlowski, Jpn. J. Pharmacol. 32 (1982) 1013–1017.
[24] C. Feletti, V. Bonomini, Nephron 24 (1979) 85–88.
[25] G. Andreotti, B.L. Mendez, P. Amodeo, M.A. Morelli, H. Nakamuta, A. Motta, J. Biol. Chem. 281 (2006) 24193–24203.
[26] F.R. Singer, J.P. Aldred, R.M. Neer, S.M. Krane, J.T. Potts, K.J. Bloch, J. Clin. Invest. 51 (1972) 2331–2338.
[27] J.F. Habeber, F.R. Singer, L.J. Deftos, J.T. Potts JR., Endocrinology 90 (1972) 952–960.
[28] A. Cudd, T. Arvinte, R.E. Gaines Das, C. Chinni, I. MacIntyre, J. Pharm. Sci. 84 (1995) 717–719.
[29] M. Faller, M. Matsunaga, S. Yin, J.A. Loo, F. Guo, Nat. Struct. Mol. Biol. 14 (2007) 23–29.
[30] S. Hou, M.F. Reynolds, F.T. Horrigan, S.H. Heinemann, T. Hoshi, Acc. Chem. Res. 39 (2006) 918–924.
[31] D. Chiabrando, F. Vinchi, V. Fiorito, S. Mercurio, E. Tolosano, Front. Pharmacol. 5 (2014) 1–24.
[32] L.L. Yin, H. Yuan, K.J. Du, B. He, S.Q. Gao, G.B. Wen, X. Tan, Y.W. Lin, Chem. Commun. 54 (2018) 4356–4359.
[33] J.B. Cannon, J. Pharm. Sci. 82 (1993) 435–446.
[34] E.Y. Hayden, P. Kaur, T.L. Williams, H. Matsui, S.R. Yeh, D.L. Rousseau, Biochem 54 (2015) 4599–4610.
[35] Y. Liu, J.A. Carver, L.H. Ho, A.K. Elias, I.F. Musgrave, T.L. Pukala, Biochem. Biophys. Res. Commun. 454 (2014) 295–300.
[36] J. Wu, J. Zhao, Z. Yang, H. Li, Z. Gao, Chem. Res. Toxicol. 30 (2017) 1711–1719.
[37] M. Masuda, N. Suzuki, S. Taniguchi, T. Oikawa, T. Nonaka, T. Iwatsubo, S. Hisanaga, M. Goedert, M. Hasegawa, Biochem 45 (2006) 6085–6094.
[38] C. Yuan, Z. Gao, Chem. Res. Toxicol. 26 (2013) 262–269.
[39] H. Ye, Z. Yang, H. Li, Z. Gao, Dalton Trans. 46 (2017) 10315–10323.
[40] H. Atamna, K. Boyle, Proc. Natl. Acad. Sci. U. S. A. 103 (2006) 3381–3386.
[41] S. Mukherjee, S.G. Dey, Inorg. Chem. 52 (2013) 5226–5235.
[42] E.M. Harvat, C. Redfield, J.M. Stevens, S.J. Ferguson, Biochem 48 (2009) 1820–1828.
[43] M. Paoli, J. Marles-Wright, A. Smith, DNA Cell Biol. 21 (2002) 271–280.
[44] D. Clarisse, G. Robert, I.P. Nadia, L. Sylvie, D. Muriel, W. Cécile, B. Claudette, L. Anne, Biochem 42 (2003) 10627–10633.
[45] S. Hofbauer, A. Hagmüller, I. Schaffner, G. Mlynek, M. Krutzler, G. Stadlmayr, K.F. Pirker, C. Obinger, H. Daims, K. Djinović-Carugo, Arch. Biochem. Biophys. 574 (2015) 36–48.
[46] L. Peter, Z. Jing, F. Stefan, Biochem 53 (2015) 6863–6877.
[47] L. Rivillas-Acevedo, C. Sanchez-Lopez, C. Amero, L. Quintanar, Inorg. Chem. 54 (2015) 3788–3796.
[48] A. Kapurniotu, J.W. Taylor, J. Med. Chem. 38 (1995) 836–847.
[49] Y. Zhou, J. Wang, L. Liu, R. Wang, X. Lai, M. Xu, ACS Chem. Neurosci. 4 (2013) 535–539.
[50] H. Ye, H. Li, Z. Gao, Chem. Res. Toxicol. 31 (2018) 904–913.
[51] H.N. Little, J.B. Neilands, Nature 188 (1960) 913–915.
[52] M. Paoli, B.F. Anderson, H.M. Baker, W.T. Morgan, A. Smith, E.N. Baker, Nat. Struct. Biol. 6 (1999) 926–931.
[53] G. Andreotti, R.M. Vitale, C. Avidan-Shpalter, P. Amodeo, E. Gazit, A. Motta, J. Biol. Chem. 286 (2011) 2707–2718.
[54] A. Sinopoli, A. Magri, D. Milardi, M. Pappalardo, P. Pucci, A. Flagiello, J.J. Titman, V.G. Nicoletti, G. Caruso, G. Pappalardo, G. Grasso, Metallomics 6 (2014) 1841–1852.
[55] A. Abedini, F. Meng, D.P. Raleigh, J. Am. Chem. Soc. 129 (2007) 11300–11301.
[56] H. LeVine, Methods Enzymol. 309 (1999) 274–284.
[57] X. Fu, X. Zhang, Z. Chang, Biochem. Biophys. Res. Commun. 329 (2005) 1087–1093.
[58] S. Arya, A. Kumari, V. Dalal, M. Bhattacharya, S. Mukhopadhyay, Phys. Chem. Chem. Phys. 17 (2015) 22862–22871.
[59] K.K. Sweers, K.O. van der Werf, M.L. Bennink, V. Subramaniam, ACS Nano 6 (2012) 5952–5960.
[60] A. Kapurniotu, R. Kayed, J.W. Taylor, W. Voelter, Eur. J. Biochem. 265 (1999) 606–618.
[61] M.A. Kumar, E. Slack, A. Edwards, H. Soliman, A. Baghdiantz, G. Foster, I. MacIntyre, J. Endocrinol. 33 (1965) 469–475.
[62] B. Cheng, H. Gong, H. Xiao, R.B. Petersen, L. Zheng, K. Huang, Biochim. Biophys. Acta 1830 (2013) 4860–4871.
[63] B. Bulic, M. Pickhardt, B. Schmidt, E.M. Mandelkow, H. Waldmann, E. Mandelkow, Angew. Chem. Int. Ed. 48 (2009) 1740–1752.
[64] C. Guo, L. Ma, Y. Zhao, A. Peng, B. Cheng, Q. Zhou, L. Zheng, K. Huang, Sci. Rep. 5 (2015) 13556.
[65] F.I. Baptista, A.G. Henriques, A.M. Silva, J. Wiltfang, O.A. da Cruz e Silva, ACS Chem. Neurosci. 5 (2014) 83–92.
[66] R. Khodarahmi, F. Naderi, A. Mostafaie, K. Mansouri, Arch. Biochem. Biophys. 494 (2010) 205–215.
[67] C. Iannuzzi, S. Vilasi, M. Portaccio, G. Irace, I. Sirangelo, Protein Sci. 16 (2007) 507–516.
[68] M. Reches, Y. Porat, E. Gazit, J. Biol. Chem. 277 (2002) 35475–35480.
[69] N. Rezaei-Ghaleh, M. Amininasab, M. Nemat-Gorgani, Biophys. J. 95 (2008) 4139–4147.
[70] C. Wu, H. Lei, Z. Wang, W. Zhang, Y. Duan, Biophys. J. 91 (2006) 3664–3672.
[71] A. Bertolani, A. Pizzi, L. Pirrie, L. Gazzera, G. Morra, M. Meli, G. Colombo, A. Genoni, G. Cavallo, G. Terraneo, P. Metrangolo, Chemistry 23 (2017) 2051–2058.
[72] H. Itoh-Watanabe, M. Kamihira-Ishijima, N. Javkhlantugs, R. Inoue, Y. Itoh, H. Endo, S. Tuzi, H. Saito, K. Ueda, A. Naito, Phys. Chem. Chem. Phys. 15 (2013) 8890–8901.
[73] A. Naito, M. Kamihira, R. Inoue, H. Saito, Magn. Reson. Chem. 42 (2004) 247–257.
[74] A. Shtainfeld, T. Sheynis, R. Jelinek, Biochem 49 (2010) 5299–5307.
[75] R. Huang, S. Vivekanandan, J.R. Brender, Y. Abe, A. Naito, A. Ramamoorthy, J. Mol. Biol. 416 (2012) 108–120.
[76] D. Pramanik, S.G. Dey, J. Am. Chem. Soc. 133 (2011) 81–87.
[77] V. Bondarenko, S. Dewilde, L. Moens, G.N. La Mar, J. Am. Chem. Soc. 128 (2006) 12988–12999.
[78] I. Bertini, C. Luchinat, J.M. Li, M. Piccioli, M. Sola, J.S. Valentine, Inorg. Chem. 31 (1992) 4433–4435.